A Comparison of the Isothermal Fatigue Behavior of Sn-Ag-Cu to Sn-Pb Solder

Nathan Blattau and Craig Hillman
DfR Solutions
College Park, Maryland

Abstract
The movement to Pb-free soldering will result in solder joints that are significantly stiffer than those made of SnPb. This paper presents the results from the first phase of a two-part study to understand and compare the isothermal mechanical fatigue behavior of tin-silver-copper (SnAgCu) solder to that of tin-lead (SnPb) solder. A combination of experiments and finite element analysis was used to compare and predict the durability of SnPb and SnAgCu surface mount solder joints. The experiments were composed of cyclic four-point bend tests of printed wiring board coupons populated with 2512 sized resistors at 5 and 10 Hz. This configuration was chosen so the test would reflect actual electronic products and still be rapidly modeled using finite element analysis (FEA). This frequency should be sufficiently high to minimize solder creep during the testing. The board level strains were verified with strain gauges and the solder joint failures were detected using a high-speed event detector. Tests were conducted at two board level strain values and then modeled in FEA to determine the strains and stresses developed in the solder joint. This information was then used to determine the appropriate cyclic fatigue relationship for both SnAgCu and SnPb solder. The results indicate that at high board level strains SnPb solder out performs SnAgCu solder. However, at lower board level strains the SnAgCu solder out performed SnPb. The second phase of the study involves bend testing at even lower board level strains to characterize the high cycle fatigue behaviors of the solders.

Key words: solder joints, fatigue, bending, flex

Introduction
The impact of Pb-free on the reliability of electronic assemblies is of great concern to the industry. While many studies have been done to address the reliability during thermal cycling of tin-silver-copper (SAC) solder, few studies have addressed the durability during mechanical fatigue. The purpose of this study is to develop a better understanding of the fatigue behavior of SnAgCu solder joints during mechanical cycling.

Sample Population
The resistor size selected for testing was 2512 and is a Pb-free part, having terminations that are 100% tin. To prevent lead contamination, the board finish selected for this study was electroless nickel - immersion gold (ENIG). Test boards for the 2512 size resistors were assembled using Sn3.0Ag0.5Cu (SAC 305) and Sn63Pb37 solder. Summaries of the sample types are shown in
Table 1.

Table 1 - Capacitors and Solder Compositions

Size	Solder Composition	Board Strain (με)	Coupons
2512	SnPb	800	1
2512	SnPb	1200	1
2512	SnPb	2400	1
2512	SnAgCu	800	1
2512	SnAgCu	1200	1
2512	SnAgCu	2400	2

The test coupons for the assemblies are shown in Table 2. Each coupon holds 40 resistors and was tested at the board level strain values shown in
Table 1.

Experimental Procedure

The test coupons were tested at the University of Maryland, Baltimore County - Laboratory for Advanced Manufacturing and Production using a Bose EnduraTEC Elf 3300 tester shown in
Figure 1. The Elf 3300 uses a hybrid design that includes an electromagnetic linear motor and a pneumatic static load stage. The system can do static, dynamic and fatigue tests at loads up to 4.5 kN and at frequencies as high as 100 Hz.

Table 2 - Resistor Test Coupons

2512 - SnAgCu	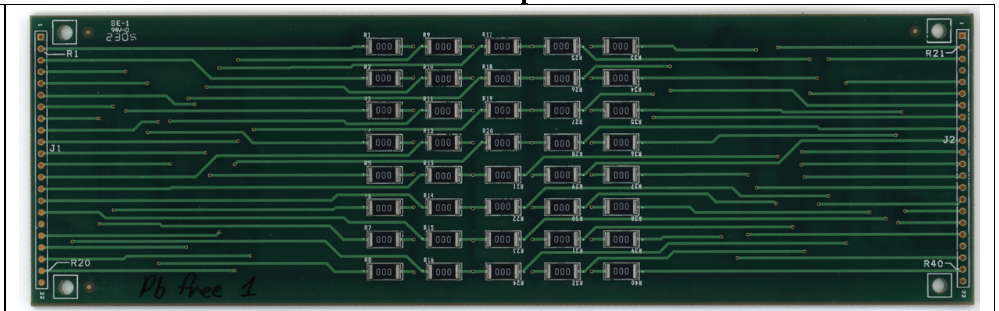
2512 - SnPb	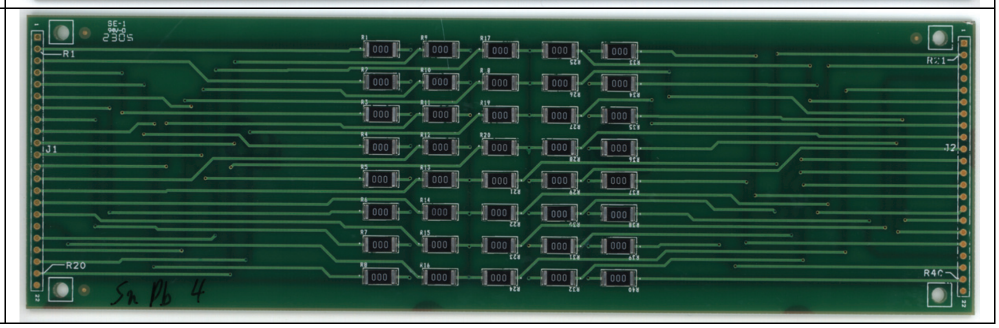

The boards were subjected to cyclic four-point bending. The maximum frequency at which the bend testing could be conducted was determined using a calibration sample of the test coupon. The test frequency was increased until the printed wiring board could no longer maintain contact with the actuator. At the 2400 and 1200 με levels this was determined to be around 5 Hz at the 800-με levels it was determined to be 10 Hz.

The four-point bend setup is shown in
Figure 2. The inner span of the fixture was 3.5 inches; the outer span was 6.5 inches. The upper support span is attached to the actuator so that its weight does not load the test coupon.

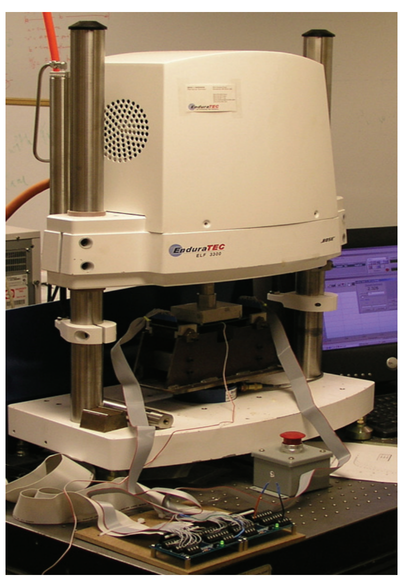

Figure 1 - EnduraTEC Elf 3300 Tester

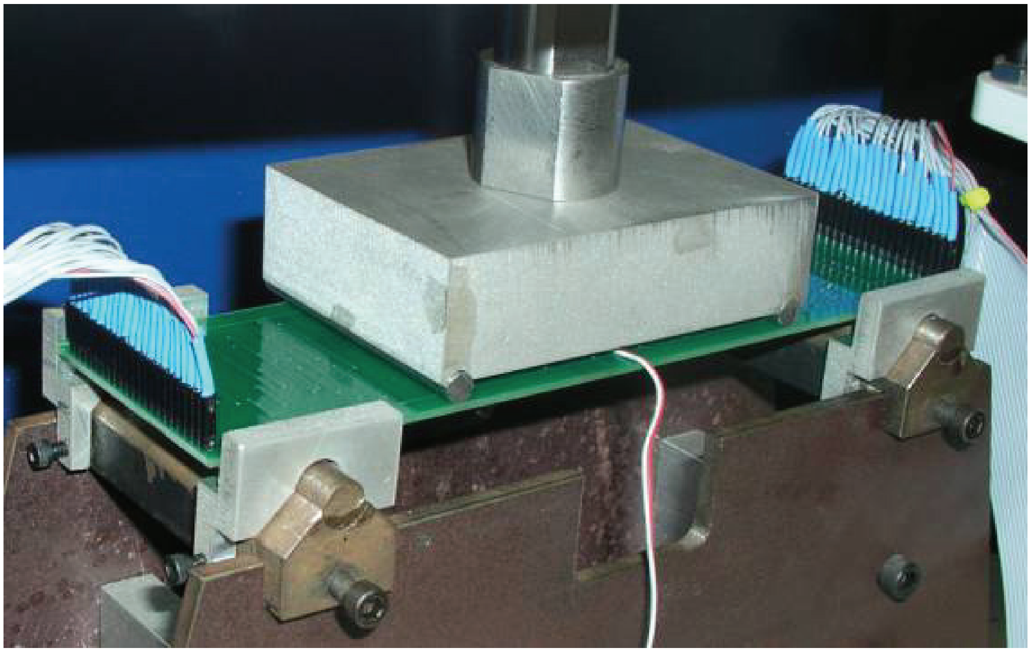

Figure 2 - Four-Point Bend Fixture and Sample

The deflections necessary to induce 800, 1200 and 2400 με were first calculated using an equation from IPC-9702 [0], ignoring the effect of the components:

$$\varepsilon = \frac{6 \cdot \delta \cdot t}{(L_2 - L_1) \cdot (L_2 + 2L_1)}$$

Equation 1

Where, ε is the global strain along the length of the board, δ is the relative displacement between the upper and lower supports, t is the PCB thickness, L_1 is the inner support span, and L_2 is the outer support span. The deflections necessary to induce the required strains were calculated to be 2.2, 3.3 and 6.6 mm respectively. The computations were then compared to the actual board level strains using a strain gauge mounted to the board, as shown in

Figure 3. The measurements indicated that the equation was adequate to predict the deflections necessary for 800 and 1200 με. However, the measured strains at 6.6 mm were 2600 με and the deflection had to be reduced to 6.2 mm to achieve 2400 με.

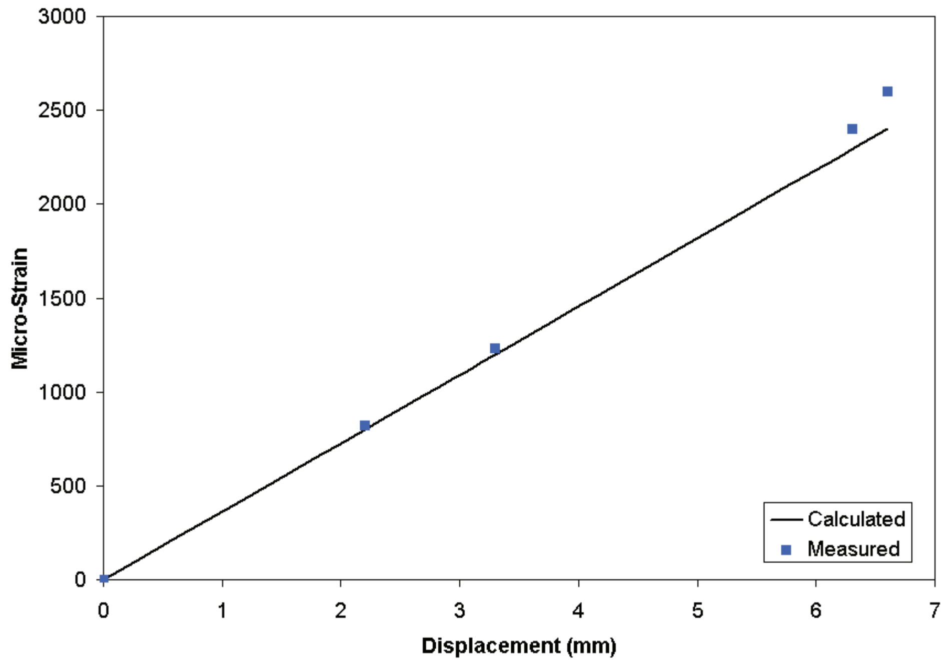

Figure 3 - Comparison Between Measured and Calculated Board Level Strains

A low-cost custom event detector that is composed of comparators, data latches and a digital input module was used to record the cycles to failure for each resistor. The detection window was less than 0.1 mS and the threshold resistance was set to 300 ohms. A custom software program was developed to interface to the event detector. This software recorded the time required to have 10, 20 and 30 events on each component. Once each component accumulated 500 events the software no longer monitored that device. After all components failed the software terminated the monitoring and provided feedback to the operator indicating that the test could be stopped. An example of the software interface is shown in
Figure 4. Darkened indicators designate devices that have accumulated more than 500 failure events.

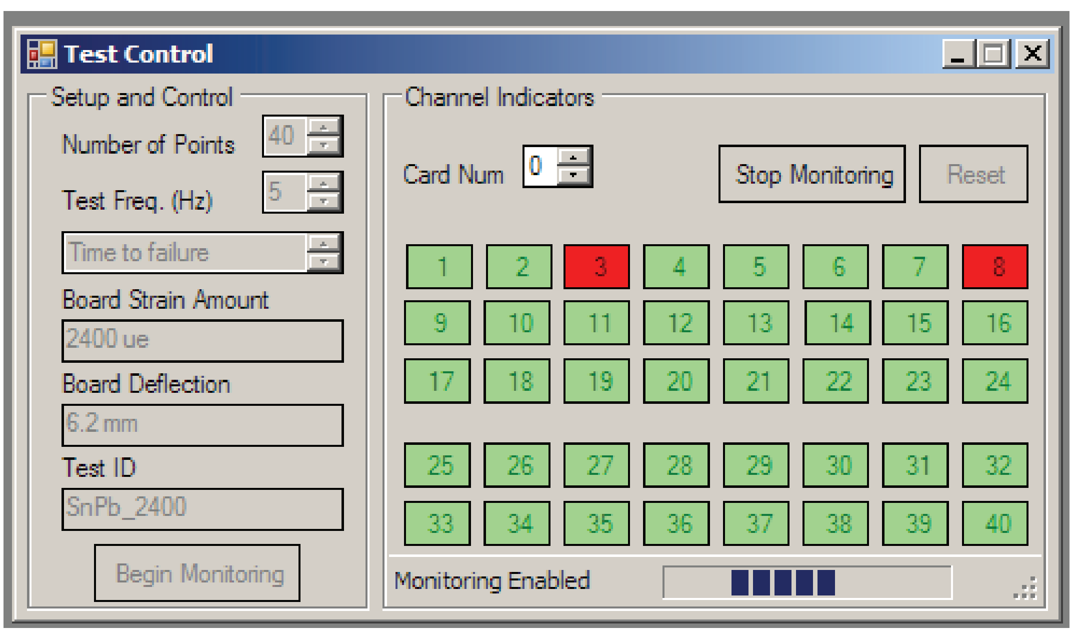

Figure 4 - Test Monitoring Software Interface

Results

Three tests were conducted at board level strains of 2400 $\mu\varepsilon$, one for SnPb and two for SnAgCu. The results of the tests at 2400 $\mu\varepsilon$ are shown graphically as 2-parameter Weibull plots in

Figure 5. The results show that at high strain, the SnPb solder out performs the SnAgCu solder. The characteristic life of the SnPb solder was 19500 cycles, the characteristic life of the two tests of the SnAgCu were 7730 and 10500 cycles.

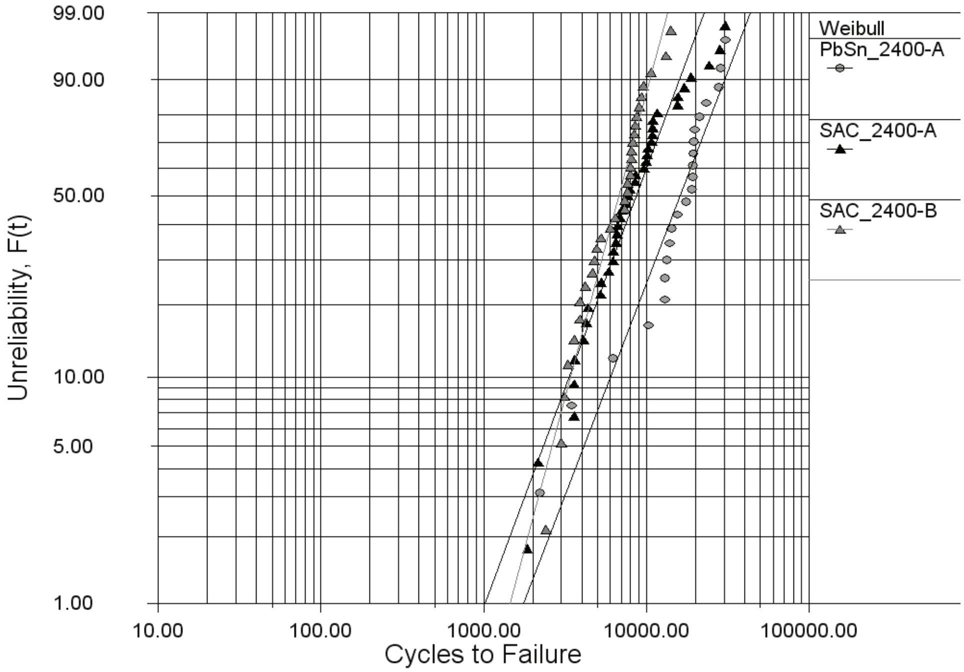

β1=1.9122, η1=1.9485E+4, ρ=0.9559
β2=1.9716, η2=1.0508E+4, ρ=0.9709
β3=2.7480, η3=7732.8259, ρ=0.9781

Figure 5 - Failure Fata at 2400 με, SnPb and SnAgCu

The results for the two tests conducted at 1200 με are shown in
Figure 6. These results indicate that as the board level strains decrease the SnAgCu solder has better fatigue properties than the SnPb solder. The characteristic life of the SnPb was 69400 cycles and the characteristic life of the SnAgCu was 264000 cycles.

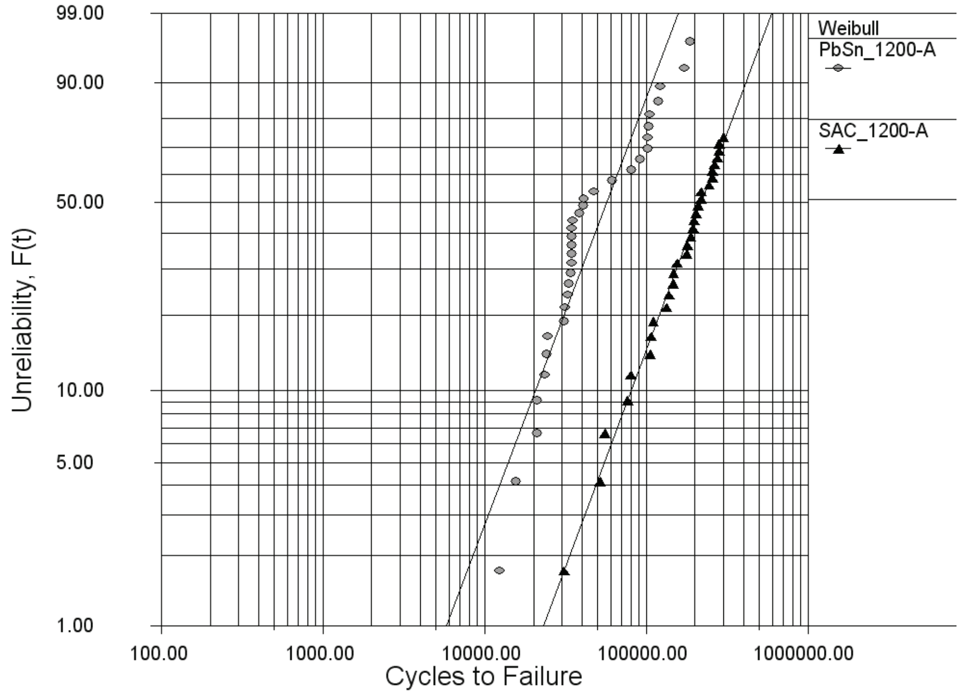

β1=1.8525, η1=6.9399E+4, ρ=0.9382
β2=1.8844, η2=2.6395E+5, ρ=0.9967

Figure 6 - Failure Data at 1200 με, SnPb and SnAgCu

The results for the two tests conducted at 800 με are shown in Figure 7. These results indicate that as the board level strains decreases even further the advantages of SnAgCu solder over SnPb solder decreases slightly. The characteristic life of the SnPb was 1,870,000 cycles and the characteristic life of the SnAgCu was 2,930,000 cycles.

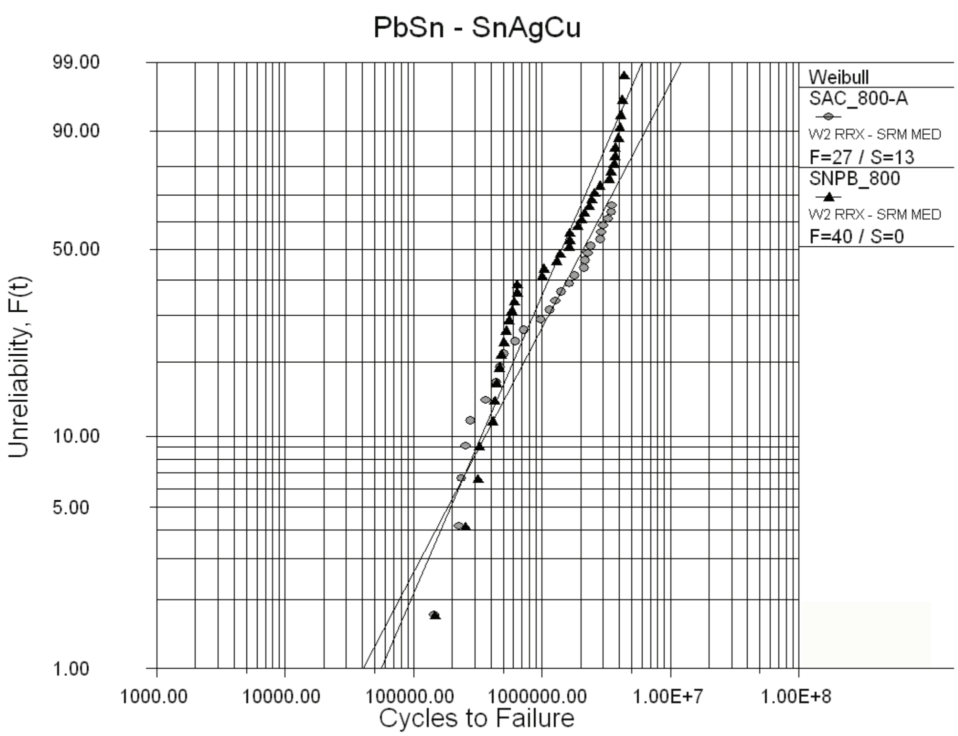

β1=1.0759, η1=2.9293E+6, ρ=0.9618
β2=1.3124, η2=1.8708E+6, ρ=0.9629

Figure 7 - Failure Data at 800 με, SnPb and SnAgCu

The tested boards were then subjected to failure analysis to verify the failure mode.

Failure Analysis

Cross sectioning of the resistors was done to identify the failure site and to compare the SnPb to the SnAgCu failures.

1. SnPb

A failed resistor with SnPb solder is shown in

Figure 8. At this magnification the failure is not clearly evident. However, grain coarsening at the toe of the solder joint indicates that it may be an area of high stress.

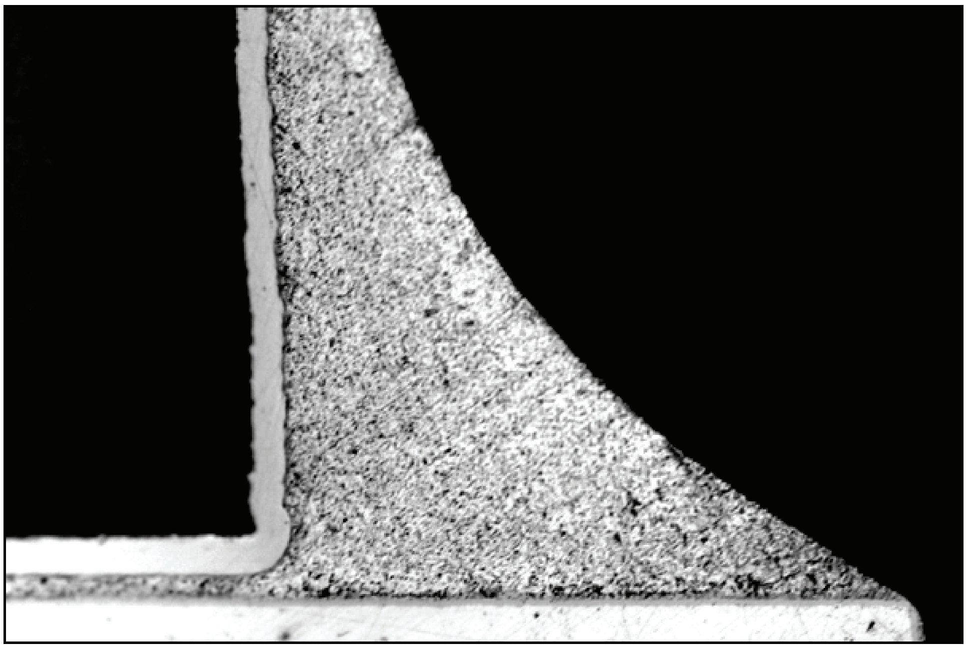

Figure 8 - SnPb, Failed Solder Joint, 200X

A higher magnification image is shown in

Figure 9 and clearly shows a crack along the bond pad just above the intermetallics.

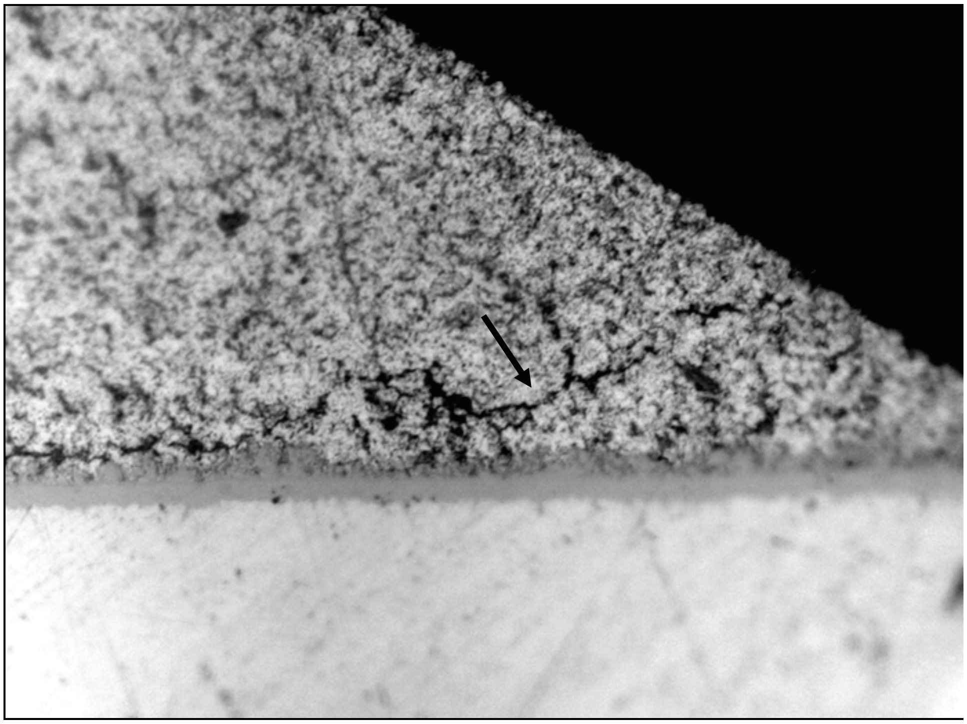

Figure 9 - SnPb, Fatigue Crack, 1000X

The crack appears to originate from the toe of the solder joint and then propagates towards the component, as depicted in Figure 10. This crack path was confirmed by the observation of partial cracks that did not propagate underneath the component.

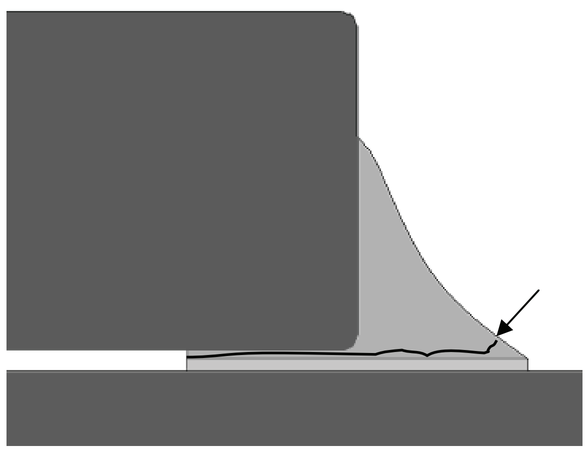

Figure 10 - Crack Initiation Site and Path

The failure site was identical regardless of the board level strain tested (800, 1200 or 2400 $\mu\varepsilon$).

2. SnAgCu

A failed resistor with SnAgCu solder is shown in Figure 11. The SnAgCu solder joint failures were much easier to identify. In Figure 11 the crack starts in the toe fillet and propagates inward. The crack initiates much further up the fillet than in the SnPb solder joints and the initiation site appears to correspond to a shrinkage crack. This is more clearly shown in Figure 12, which is a cross section of another failed SnAgCu resistor.

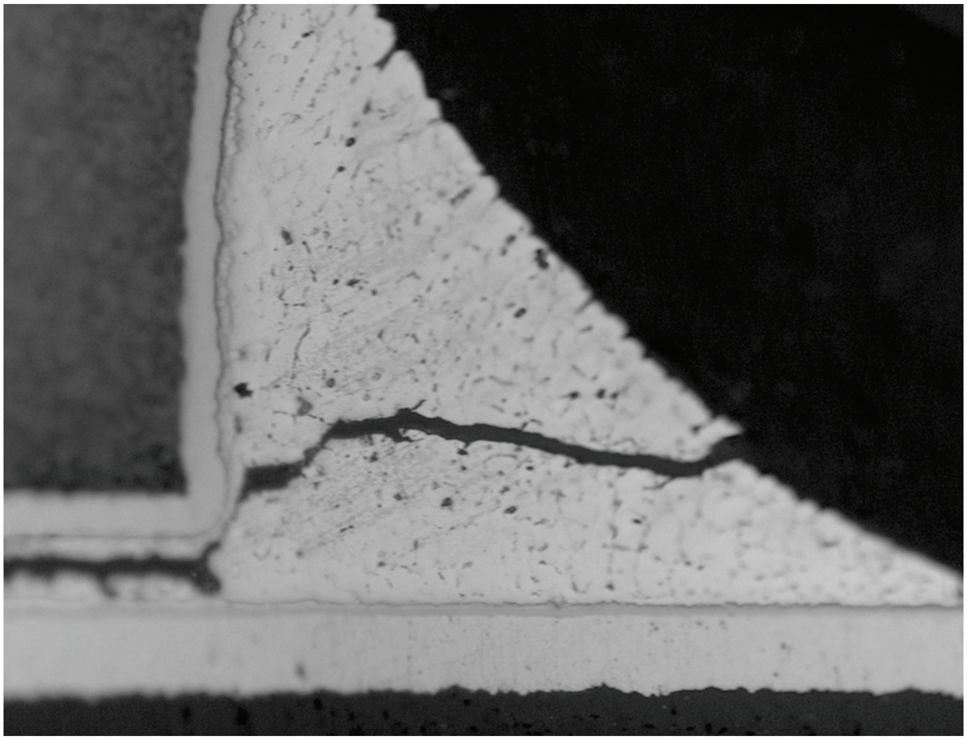

Figure 11 - SnAgCu, Failed Solder Joint, 200X

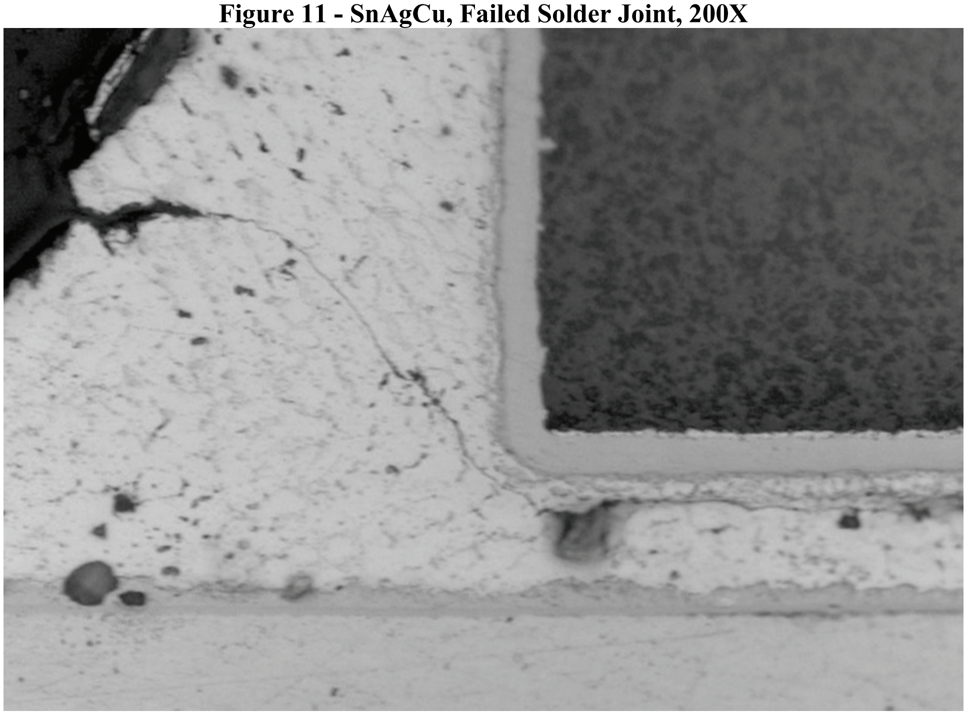

Figure 12 - SnAgCu, Failed Solder Joint, 200X

A higher magnification image of the shrinkage cracks and the fatigue crack is shown in Figure 13.

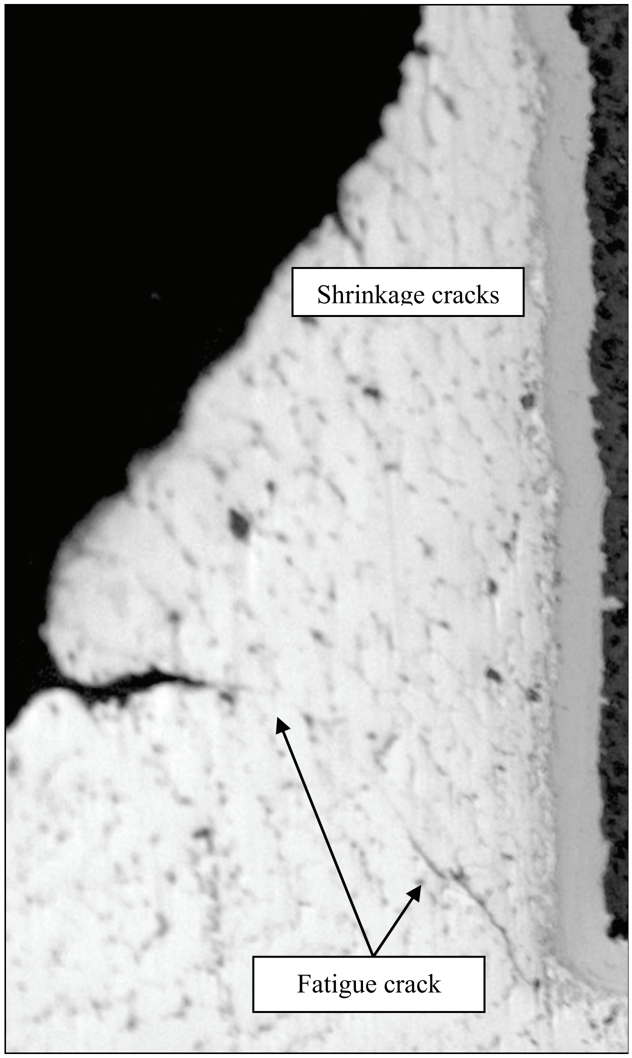

Figure 13 - Shrinkage and Fatigue Cracks, 500X

Finite Element Modeling

Finite element modeling was conducted to determine the stresses and strains developed in the solder joint during the bend testing. The analysis and modeling was done using Abaqus CAE version 6.5-1. The material properties for the solders were assumed to be multi-linear [4] and are shown in Table 3, which corresponds to the stress-strain plot shown in Figure 14.

Table 3 - Multi-linear Elastic-Plastic Models for Solders [4]

SnAgCu, T [K]	**ε1**	**ε2**	**σ1 [MPa]**	**σ2 [MPa]**	**σ3 [MPa]**
278	1.4E-3	4E-3	57.4	80	2500
323	1.4E-3	4E-3	53.2	72	1900
SnPb, T [K]	**ε1**	**ε2**	**σ1 [MPa]**	**σ2 [MPa]**	**σ3 [MPa]**
278	7E-4	3E-3	21	41	600
323	7E-4	3E-3	19	31	400

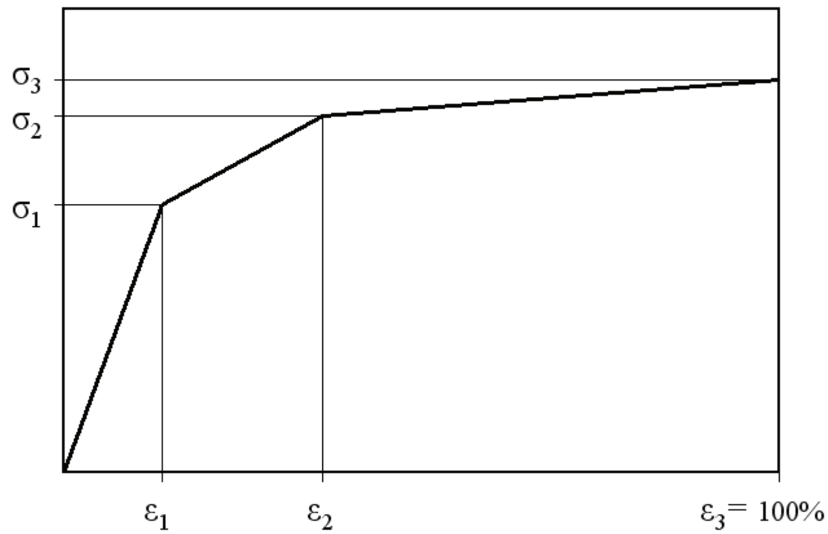

Figure 14 - Elastic-Plastic Model for FEA [4]

The properties of the printed wiring board (FR-4), copper and resistor body (alumina) are shown in Table 4. The copper bond pad was assumed to be elastic and perfectly plastic at its yield stress of 120 MPa.

Table 4 - Mechanical Properties of Copper, Alumina and FR-4

Material	Modulus [GPa]	Poisson's ratio	Yield Stress [MPa]
FR-4	22 x-y, 11 z	0.39 x-y, 0.11 z	-
Alumina	265	0.3	-
Copper	117	0.3	120

The model utilizes quarter symmetry and its geometry is shown in
Figure 15.

The printed wiring board had a bending moment applied to the end using MPC (multi-point constraints) so that it would be subjected to pure bending. The stress and strains resulting at 500, 800, 1200 and 2400 $\mu\varepsilon$ were recorded in the area of the crack initiation site.

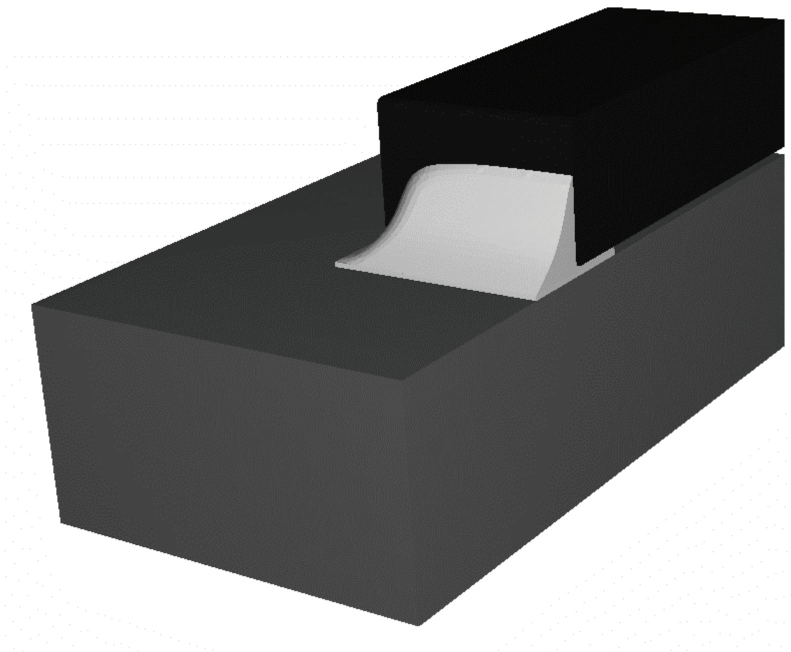

Figure 15 - 3D FEA Model of 2512 Resistor

Example fringe plots of the stress and plastic strain distributions in a SnAgCu solder joint are shown in
Figure 16 and
Figure 17. The circle shown in
Figure 16 denotes the region at which the plastic strain and stresses were recorded and corresponds to the crack initiation site identified in the cross-sections.

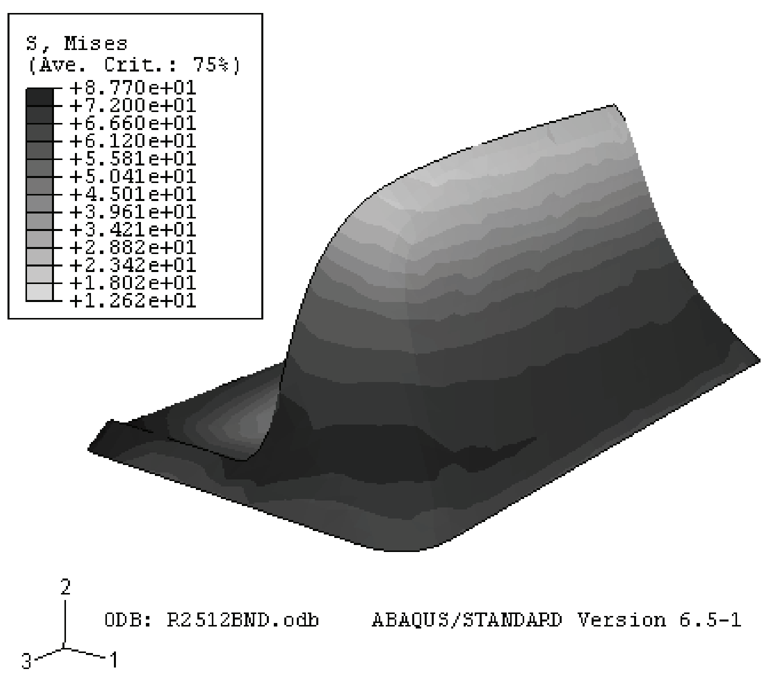

Figure 16 - Von Mises Stresses in Solder Joint (SAC)

The stress and strain results are shown in

Figure 18 as a function of board surface strain. No plastic strain was recorded for the SnAgCu model at a board level strain of 800 με.

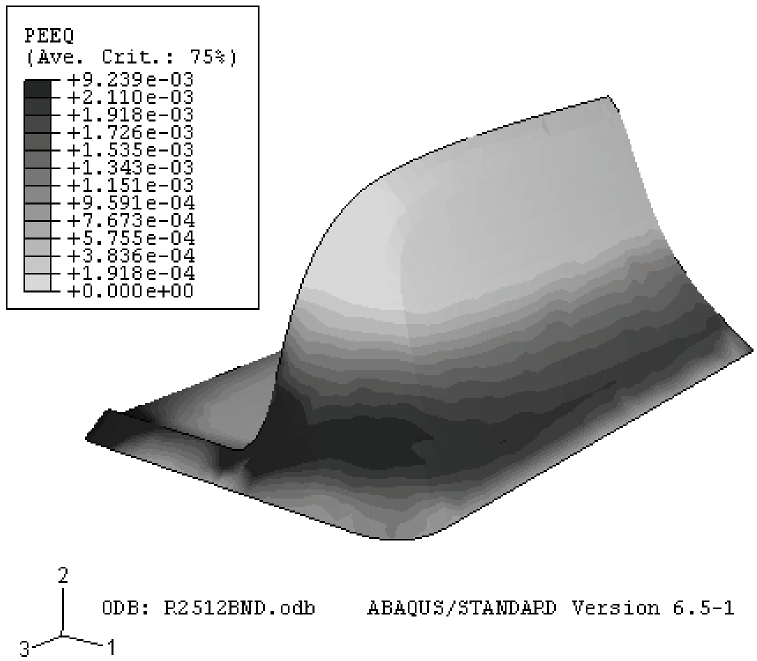

Figure 17 - Equivalent Plastic Strains in Solder Joint (SAC)

The graph shows that while the stress developed at the crack initiation site is non-linear as a function of board bending the plastic strains developed in that same region are linear as a function of board bending.

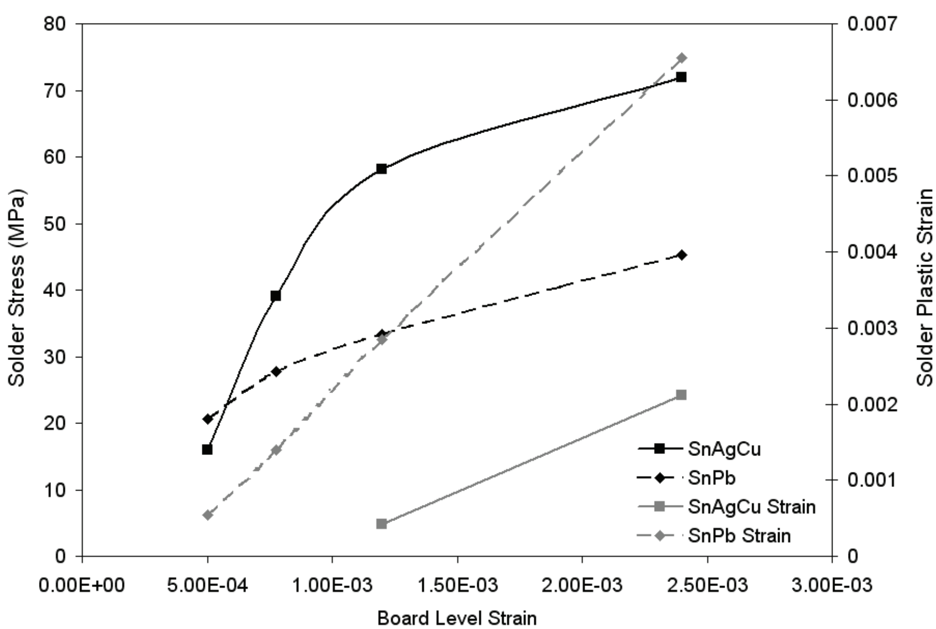

Figure 18 - Stress and Strain Results

This data and the experimental results can now be used to develop a fatigue equation based upon relationships developed by Coffin-Manson [5].

$$N_f(50\%) = \frac{1}{2}\left(\frac{2\varepsilon_f'}{\Delta\gamma_p}\right)^{-\frac{1}{c}}$$

Equation 2: Low-cycle fatigue equation [5]

Where:
N_f =number of cycles to failure
ε_f = fatigue ductility coefficient,
c = the fatigue ductility exponent, -0.5 to -0.7 for common engineering metals.
$\Delta\gamma_p$ = the cyclic plastic strain range.

Preliminary fatigue predictions were made using the fatigue ductility exponent (c = –0.6) suggested by Engelmaier [6] for test frequencies greater than 0.5 Hz, However this underestimated the cycles to failure for the SnPb solder and the value of –0.442 [6] for c provided a much better prediction. This exponent was then modified so that the equation adequately predicted the life of the SnAgCu solder joints. This yielded a fatigue ductility exponent of – 0.57.

Table 5 - Coffin-Manson Parameters

Material	ε_f	c
SnPb	0.325	– 0.442
SnAgCu	0.325	– 0.57

The cycle to failure predictions and the experimental test results are shown in plotted in Figure 19.

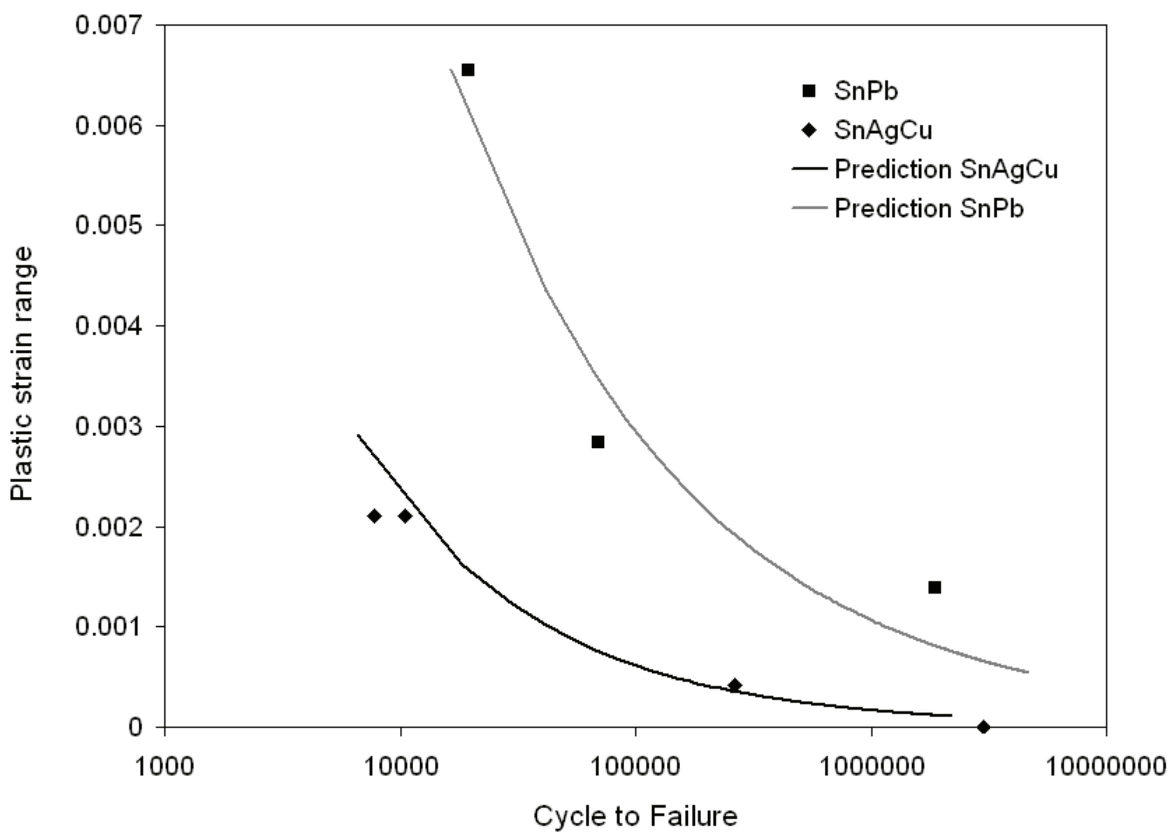

Figure 19 - Coffin-Manson Fatigue Predictions

Conclusion

Experimental results at very high board level strains indicate that SnPb solder outperforms Pb-free solder. This seems to correlate with severe thermal cycling experiments. However, there is a crossover point at which SAC out performs SnPb.

This crossover point occurs at a relatively high board level strain between 2400 and 1200 με. These strains are much higher than those one would expect to encounter in the actual use of electronic systems since they would cause failures in other components, such as ceramic chip capacitors. Experiments conducted at board level strains of 800 με indicate that at this board level strain the average fatigue life of SAC is around 3 million cycles.

The failure analysis of the solder joints highlights the difference in the crack morphology between SAC and SnPb. Cracks in the SnPb joints were very small and associated with grain coarsening and secondary micro-cracks. The cracks in the SAC solder joints were well defined and had a distinct crack path that appears to initiate at a shrinkage crack.

The isothermal mechanical cycling fatigue equations using the plastic strain range of the solder at the crack initiation site have also been presented. The fatigue relationship for SnPb solders uses parameters provided by Engelmaier for low cycle fatigue. The fatigue ductility exponent for the SnAgCu solder had to be adjusted to -0.57, which provided an adequate fit to the test results.

The main concern over the durability of SnAgCu solder is how the presence of shrinkage cracks effect the fatigue behavior of the solder joint. If large enough, these shrinkage cracks may adversely affect the fatigue behavior of the solder. Further cross sectioning is being done to correlate early failures to the presence of large shrinkage cracks.

References

1. IPC/JEDEC 9702 Monotonic Bend Characterization of Board Level Interconnects.
2. Weibull, W., “A Statistical Distribution Function of Wide Applicability”, J. Appl. Mech., 1950, 18 293.
3. Milos Dusek, Chris Hunt, “The Measurement of Creep Rates and Stress Relaxation for Micro-sized Lead-free Solder Joints”, NPL Report DEPC MPR 021
4. S. Wiese, S. Rzepka, E. Meusel, “Time Independent Plastic Behavior of Solders and its Effect on FEM Simulations for Electronics Packages” Advanced Packaging Materials, 2002. Proceedings. 8th International Symposium on, 3-6 March 2002 Page(s): 104-111
5. Manson, S.S., Thermal Stress and Low Cycle Fatigue, McGraw-Hill, New York, 1966.
6. Engelmaier, W., "Chap. 17: Solder Attachment Reliability, Accelerated Testing, and Result Evaluation" in Solder Joint Reliability - Theory and Applications, edited by Lau, J. H., Van Nostrand Reinhold, New York, 1991, pp. 545-587.